有機伝導体 Organic Conductors

導伝性高分子: Polymers with conjugated π-electron systems

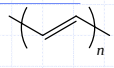

polyacetylene

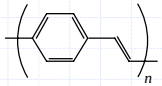

poly(phenylenevinylene)
PPV

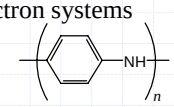

polyaniline

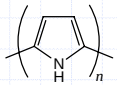

polypyrrole

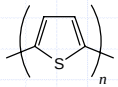

polythiophene

phthalocyanine CuPc

低分子 Small Molecules

有機半導体 Organic Semiconductors

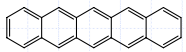

pentacene

電荷移動錯体 Charge-transfer salts

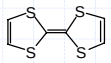

tetrathiafulvalene
TTF

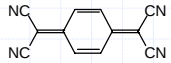

tetracyanoquionodimethane
TCNQ

One chain truncated from graphite (terminated by hydrogenes)
→ Polyacetylene

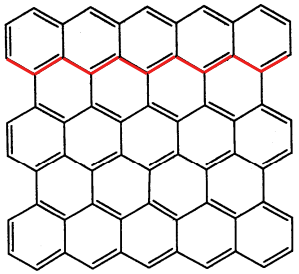

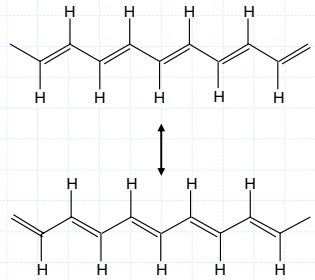

Electrically conducting because the p-electrons can move.

半導体 Semiconductor

白川英樹 2000年 Nobel Prize
H. Shirakawa

Doped Polyacetylene

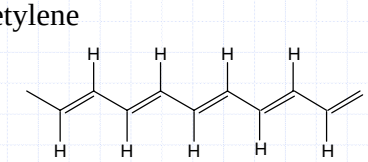

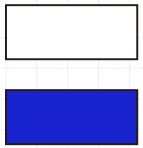

K^+

Br^-

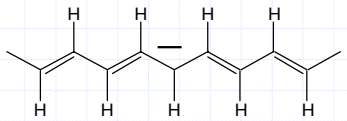

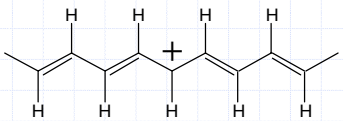

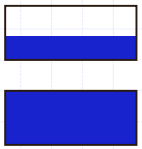

Negative

Electron dope (N型)

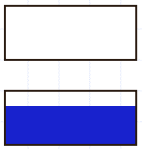

Positive

Hole dope (P型)

Graphite
(Inorganic)

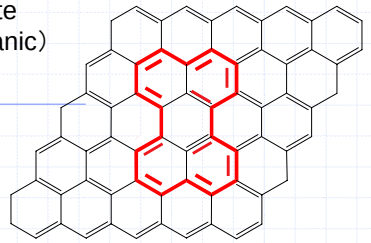

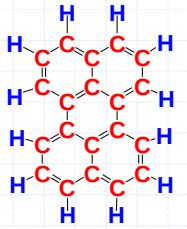

perylene

First Electrically Conducting Organics

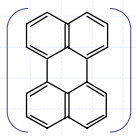

Br^-

e^-

電荷移動

Br doped Perylene shows as high electric conductivity as 0.1 Scm^{-1}.
First conducting charge-transfer salt
Akamatsu, Inokuchi, Matsunaga,
Nature, **173**, 168 (1954).

Charge-transfer complex 電荷移動錯体

Charge-transfer complex電荷移動錯体

Electron donor 電子供与体

Compounds easily oxidized to $D^0 \rightarrow D^+$ with high HOMO levels

Electron acceptor 電子受容体

Compounds easily reduced to $A^0 \rightarrow A^-$ with low LUMO levels

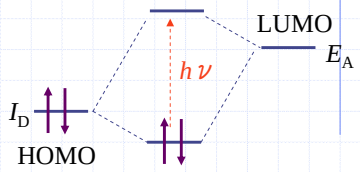

Completely $D^0A^0 \rightarrow D^+A^-$: Ionic charge-transfer complex

Nearly D^0A^0: Neutral charge-transfer complex

Small (quantum mechanical) mixing of the ionic state

$\phi = \phi(D^0A^0) + c\phi(D^+A^-)$

and the excitation corresponding to $D^0A^0 \rightarrow D^+A^-$

gives rise to charge-transfer absorption 電荷移動吸収 (visible to infrared)

$h\nu = I_D - E_A - E(D^+A^-) \backsim E_{redox}(\text{HOMO}) - E_{redox}(\text{LUMO})$

> 0.1 V D^0A^0 is more stable than D^+A^-: neutral

< 0.1 V D^+A^- is more stable than D^0A^0: ionic

Redox Potential 酸化還元電位 (cyclic voltammetry)

vs. SCE = 0.24 V NHE

Standard calomel electrode vs. Ag/AgCl = 0.22 V NHE

Ferrocene = 0.38 V vs. SCE

Energy level $= -E_{redox}(\text{vs. SCE}) - 4.4$ V

Torrance, *Mol. Cryst. Liq. Cryst.* **126**, 55 (1985).

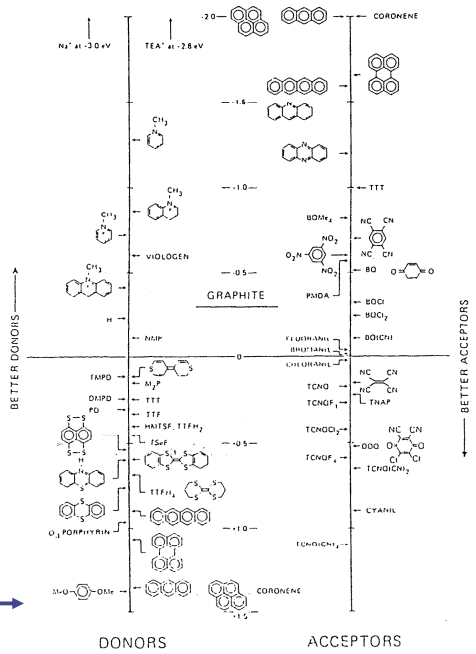

(Mixing solutions of colorless neutral donor and acceptor gives an orange to yellow solution.)

$h\nu = I_D - E_A - E(D^+A^-)$

I_D : Ionization energy of the donor

E_A : electron affinity od the acceptor

$E(D^+A^-)$: Coulomb attraction of D^+ and A^- (Madelung energy)

$h\nu = I_D - E_A - E(D^+A^-) \backsim E_{redox}(\text{HOMO}) - E_{redox}(\text{LUMO})$

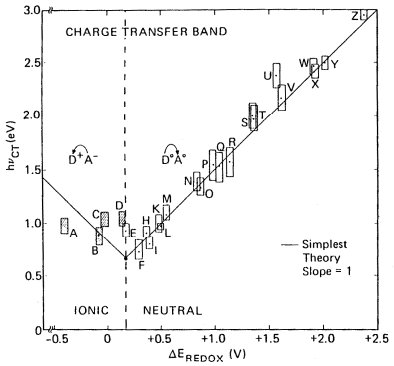

HOMO Levels

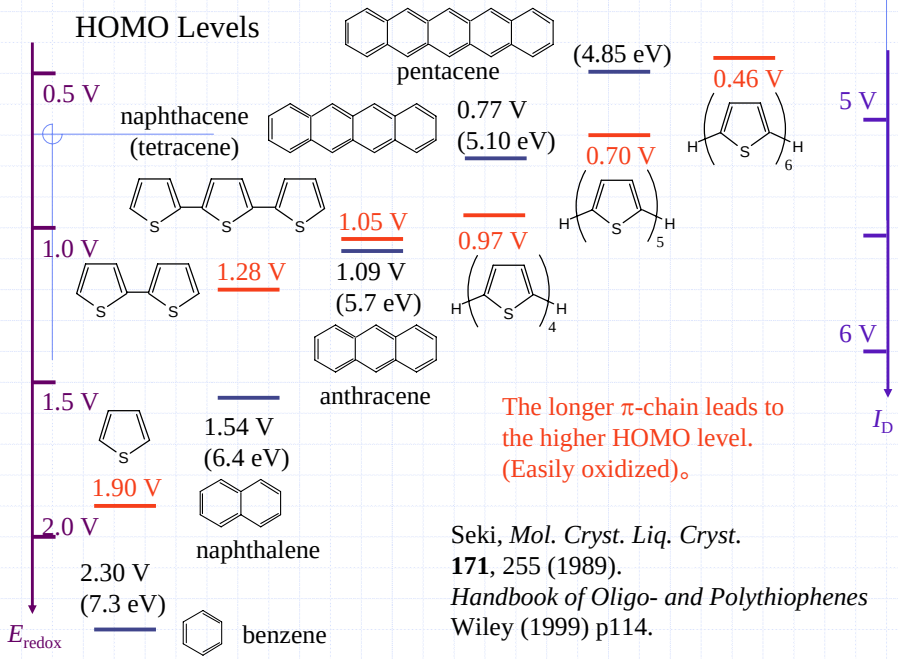

The longer π-chain leads to the higher HOMO level. (Easily oxidized)。

Seki, *Mol. Cryst. Liq. Cryst.* **171**, 255 (1989).

Handbook of Oligo- and Polythiophenes Wiley (1999) p114.

Good donors and acceptors

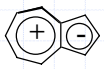

Azulene

A good donor: Tetrathiafulvalene (TTF)

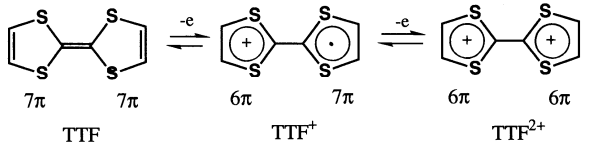

TTF TTF^{+} TTF^{2+} 0.38 V

This 7π system easily gives up one electron to form a 6π system.
(C→1π、S→2π)
Electron donating groups such as $-NH_2$, $-OCH_3$ strengthen donor ability.

A good acceptor Tetracyanoquionodimethane (TCNQ)

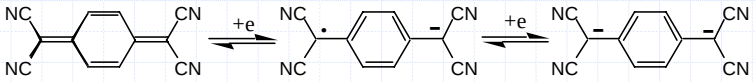

TCNQ $TCNQ^{-}$ $TCNQ^{2-}$

Reduction restores from the quinoid structure to an aromatic 6π system.
− emerges on the foot of two electron withdrawing groups (CN).
Electron withdrawing groups such as -CN、$-NO_2$ strengthen acceptor ability.

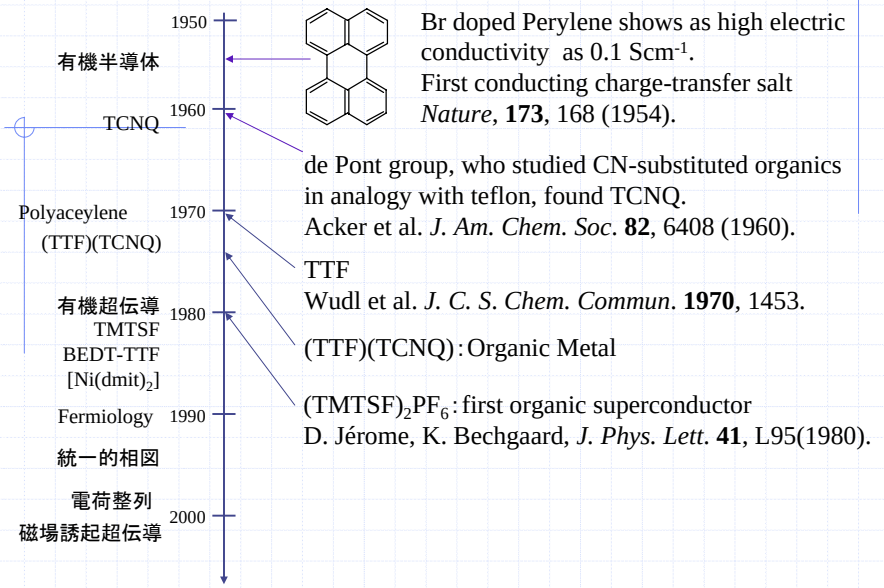

Br doped Perylene shows as high electric conductivity as 0.1 Scm^{-1}.
First conducting charge-transfer salt
Nature, **173**, 168 (1954).

de Pont group, who studied CN-substituted organics in analogy with teflon, found TCNQ.
Acker et al. *J. Am. Chem. Soc.* **82**, 6408 (1960).

TTF
Wudl et al. *J. C. S. Chem. Commun.* **1970**, 1453.

(TTF)(TCNQ): Organic Metal

$(TMTSF)_2PF_6$: first organic superconductor
D. Jérome, K. Bechgaard, *J. Phys. Lett.* **41**, L95(1980).

TCNQ complexes: stable CT complexes

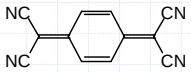

CT complexes like M(TCNQ) [M = Li, Na, K, Cu, Ag]
with conductivity 10^{-2}〜10^{-4} Scm^{-1} (semiconductor due to the 1:1 composition)

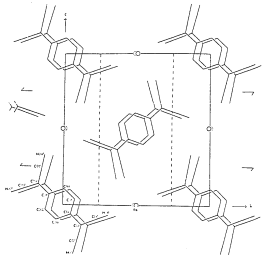

1D column structure in Rb(TCNQ)

$(TMPD^{+})(TCNQ^{-})$

TCNQ TMPD TCNQ

Mixed column structure in an ionic complex

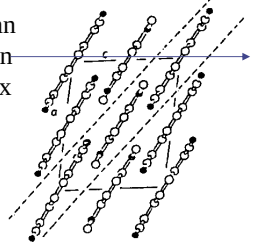

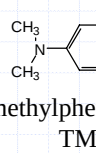

π電子

High conducting perpendicular to the molecular planes (parallel to the stacks)

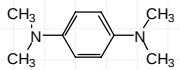

tetramethylphenylenediamine
TMPD

電子供与基: -OH、$-OCH_3$、$-NH_2$ → 電子供与体

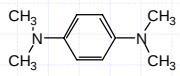

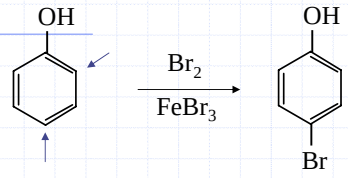

オルト、パラ配向

電子吸引基: $-NO_2$、-CN、ハロゲン、-COOH、$-COOCH_3$、-CHO

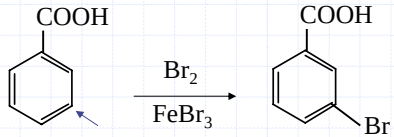

メタ配向

→ 電子受容体

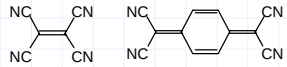

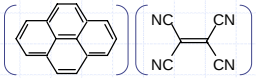

pyrene　tetracyanoethylene
TCNE

Mixed stack in a neutral complex

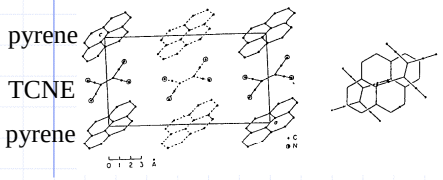

Mixed stack structure
Neutral and ionic : low conducting

Segregate stack structure
Partial charge transfer : high conducting

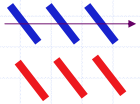

High conducting
// stack

(NMP)(TCNQ) : first「Organic Metal」1966

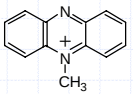

N-methylphenazinium
(NMP)

Segregated

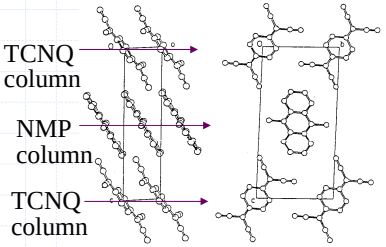

Metal at 200 K∽rt

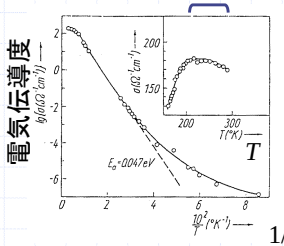

(TTF)X_x : Typical 1D Metal　(X＝Cl, Br, I, SCN, x∽0.71)

Peierls transition ⟵ non magnetic insulator below 200 K

1D stacks

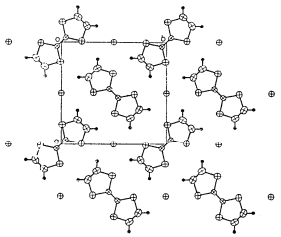

反射率:
Strongly 1D

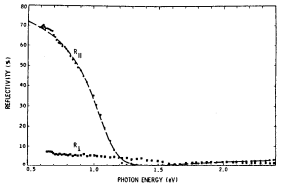

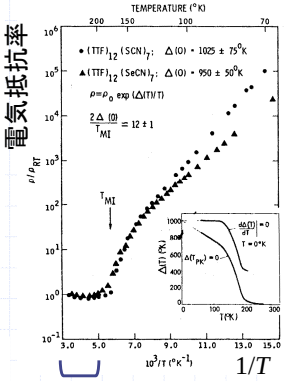

Metallic above 200 K

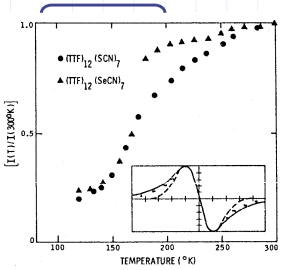

熱起電力

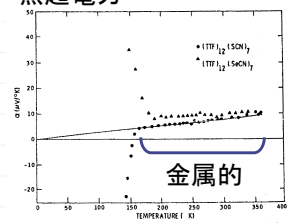

(TTF)(TCNQ)

1973

$(TTF^{0.59+})(TCNQ^{0.59-})$

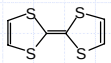

tetrathiafulvalene
TTF

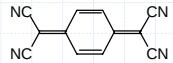

tetracyanoquionodimethane
TCNQ

拡散法結晶成長

From acetonitril
solutions of
TTF and TCNQ

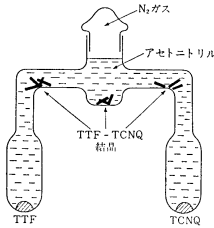

分離積層型

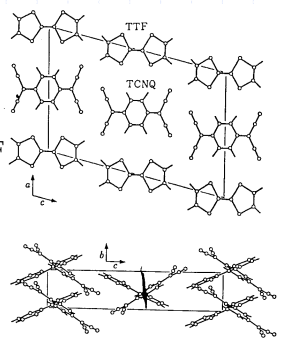

TTF

TCNQ　TCNQ

Metal at 54 K∽rt

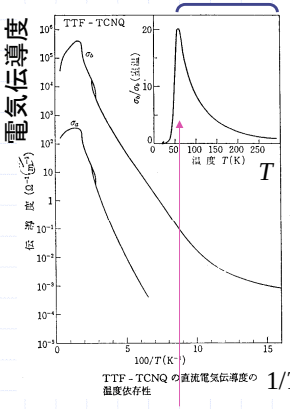

TTF - TCNQ の直流電気伝導度の温度依存性

Metal-insulator transition at 54 K

(TTF)(TCNQ)

反射率
一次元金属

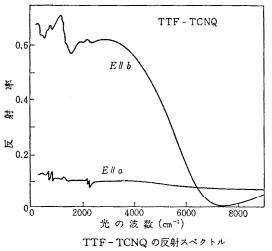

TTF - TCNQ の反射スペクトル

Energy band

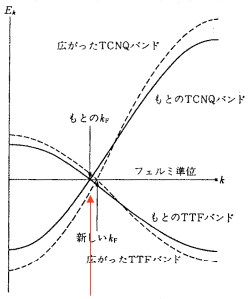

Non magnetic below 54 K

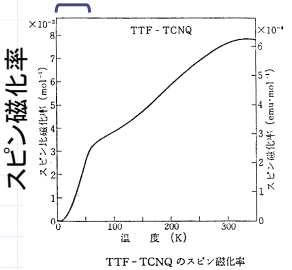

TTF - TCNQ のスピン磁化率

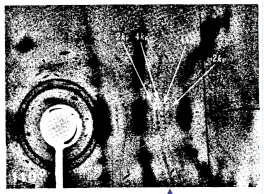

X線 : $2k_F$ periodicity

HOMO band of TTF and LUMO band of TCNQ cross each other at k_F＝0.1475b^*＝0.295π/b＝(0.59/2)(π/b)

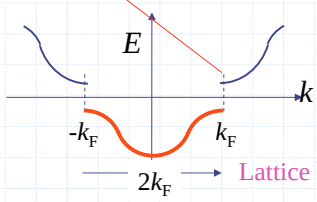

非磁性絶縁体
(Peierls転移)

Lattice has periodicity 2k_F

Different β for single and double bonds

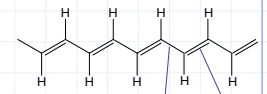

$\beta_1 = \beta_2$

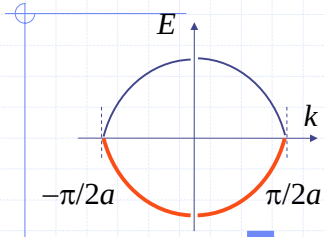

$\beta_1 \neq \beta_2$

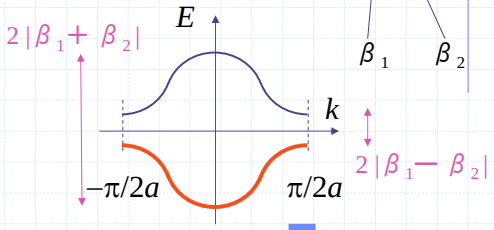

Reduced zone

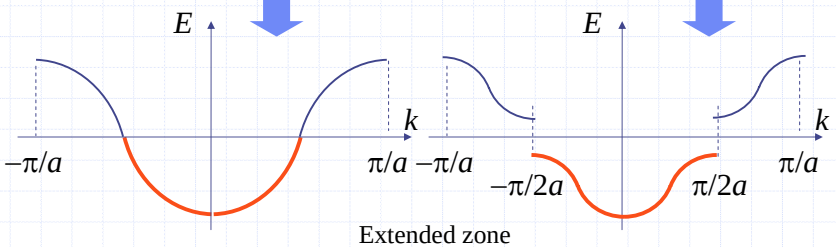

Extended zone

(TTF)(TCNQ)

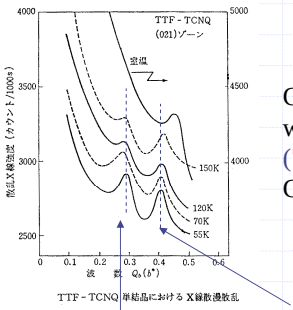

Charge has periodicity with wavelength $1/2k_F$
(電荷密度波)
Charge density wave (CDW)

$2k_F = 0.295b^*$

$4k_F = 0.59b^*$

k_F: 若干温度変化

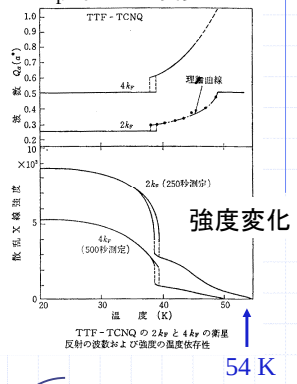

54 K

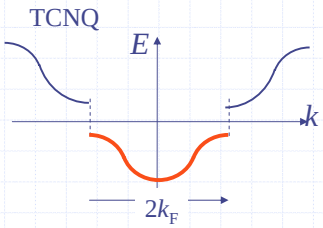

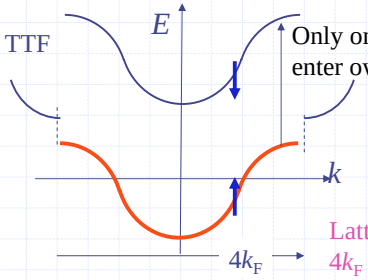

Only one electron can enter owing to U.

Lattice periodicity: $4k_F$

(TTF)(TCNQ)

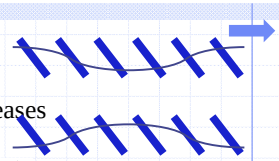

$2k_F$ changes under pressure.
"lock in" to 15 kbar above 1/3.

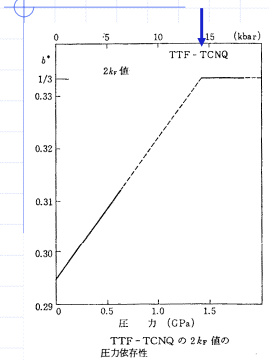

LT conductance decreases above 15 kbar.

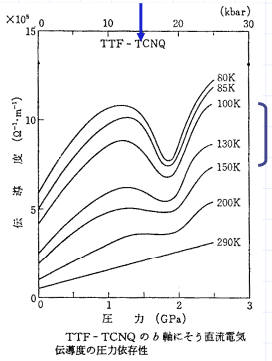

Collective motion of CDW carries current.
(CDW集団運動)
(Frölich mode)

Attempts to reduce the Peierls transition: enhance interchain interaction by Se

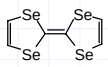

(TTF)(TCNQ) 54 K
(TSF)(TCNQ) 29 K

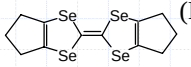

(HMTTF)(TCNQ) 50 K
(HMTSF)(TCNQ) 24 K
very little increase of R

$(TMTSF)_2PF_6$: First Organic Superconductor

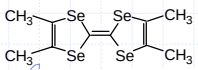

Quasi-1D Metal: Fermi surface is open, but the interchain interaction is 1/10 of the intrachain ones.

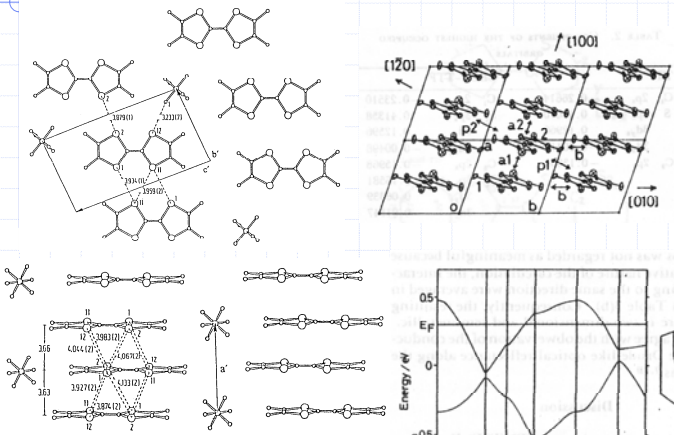

Transfer integlars (meV)

方向	HOMO
a1	200
a2	230
b	35
p1	20
p2	7

計算値 from 分子軌道計算

$(TMTSF)_2PF_6$：First Organic Superconductor

電気抵抗率

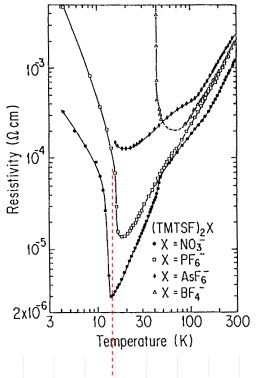

金属-半導体転移:
12 K

静磁化率

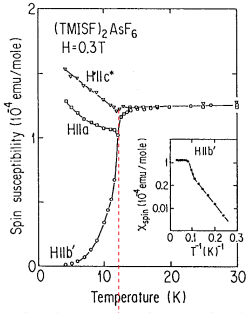

静磁化率異方性:
12 K以下

反強磁性
(spin密度波)
Spin density wave
(SDW)

圧力下相図

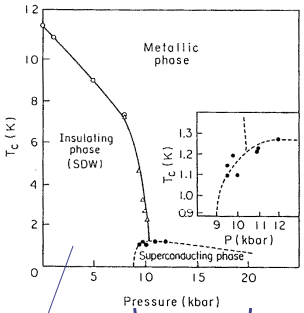

超伝導 T_c〜1 K

反強磁性(SDW)絶縁相

Experimentally distinguish origins of metal-insulator transitions

	電気抵抗率	静磁化率 (SQUID)	スピン磁化率 (ESR)	X線散乱
電荷密度波(CDW) (Peierls転移)	ρ 絶縁体 / 金属, T_{MI}, T	χ 非磁性絶縁体, T_{MI}, T	X_s the same 連続線幅 at T_{MI} $\chi \propto \frac{1}{k_B T\,(3+e^{E_g/k_B T})}$	$2k_F$長周期 > T_{MI} 散漫散乱 <T_{MI} spots
Spin密度波 (SDW)	ρ 絶縁体 / 金属, T_{MI}, T	反強磁性絶縁体 χ $\chi_\perp$ $\chi_{//}$ T_{MI}, T	線幅発散 強度→0, T	non
Mott絶縁体・電荷整列	ρ 絶縁体 / 金属, T_{MI}, T	χ 常磁性絶縁体, T_{MI}, T	The same χ_s 線幅連続 at T_{MI} SDW or spin-Peierls at lower T	Mott：non 電荷整列：長周期
Spin-Peierls転移	ρ 全温度域 絶縁体, T	χ 非磁性絶縁体, T	The same χ_s 線幅連続 at T_{MI} The same as CDW singlet-triplet model	$2k_F$の長周期

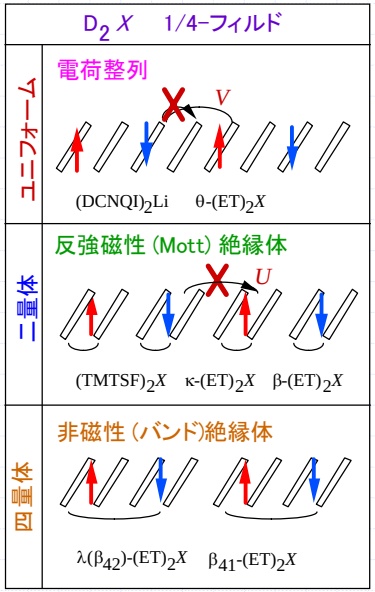

$(TMTSF)_2X$(擬一次元)系
統一的相図(Jérome相図)

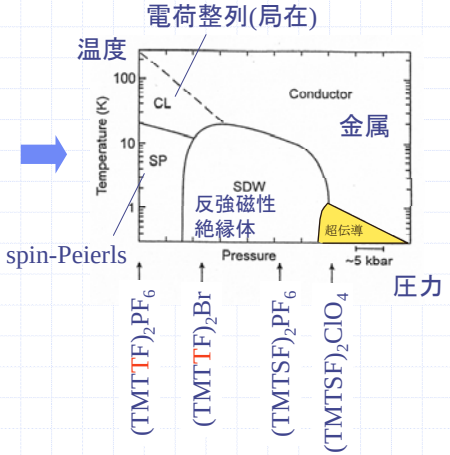

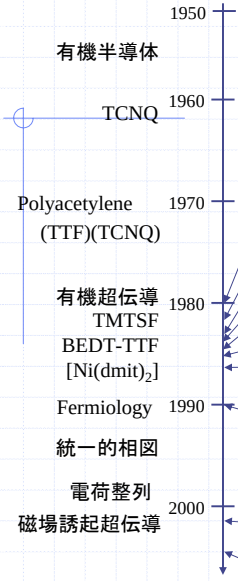

$(TMTSF)_2PF_6$：最初的有機超伝導
T_c=1.4 K (6.5 kbar) D. Jérome, K. Bechgaard 1980

$(TMTSF)_2ClO_4$：常圧有機超伝導体 T_c=1.4 K 1981

$(BEDT\text{-}TTF)_2ClO_4(TCE)$：2次元有機伝導体
G. Saito, T. Enoki, H. Kobayashi

$(BEDT\text{-}TTF)_2ReO_4$ T_c=2 K (4 kbar) 1983

β-$(BEDT\text{-}TTF)_2I_3$ T_c=1.5 K → T_c=8 K (1.2 kbar)
Yagubskii 1984 Murata, Laukhin 1985

θ-$(BEDT\text{-}TTF)_2I_3$, κ-$(BEDT\text{-}TTF)_2I_3$ H. Kobayashi

κ-$(BEDT\text{-}TTF)_2Cu(NCS)_3$ T_c=10.4 K
H. Urayama, G. Saito 1987

κ-$(BEDT\text{-}TTF)_2Cu[N(CN)_2]Br$ T_c=11.6 K
κ-$(BEDT\text{-}TTF)_2Cu[N(CN)_2]Cl$ T_c=12.8 K (0.3 kbar)
J. M. Williams 1990

λ-$(BETS)_2FeCl_4$：磁場誘起超伝導
Uji 2001

β'- $(BEDT\text{-}TTF)_2ICl_2$ T_c=14 K (82 kbar)
Taniguchi, 2003

$(BEDT\text{-}TTF)_2ClO_4(TCE)$　TCE：1,1,2-trichloroethane

G. Saito, T. Enoki, *Solid State Commun*. **42**, 557 (1982).

H. Kobayashi, et al. *J. Am. Chem. Soc*. **105**, 297 (1983).

最初的2次元有機伝導体：金属的電気伝導性@低温

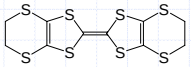

BEDT-TTF

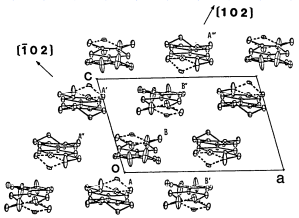

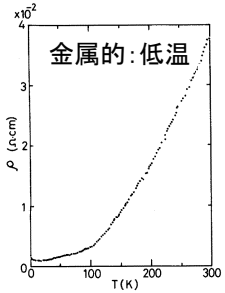

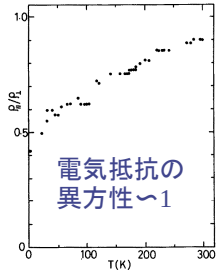

β “構造

no conductivity anisotropy

$(BEDT\text{-}TTF)_3(ClO_4)_2$ (T_{MI}＝170 K) is most easily obtained as the ClO_4 salt.

$(BEDT\text{-}TTF)_2ReO_4$

IBM Group *Phys. Rev. Lett*. 50, 270 (1983)

First Organic Superconductor of BEDT-TTF: T_c=2 K (4 kb

None can reproduce. ($(BEDT\text{-}TTF)_3(ReO_4)_2$ is the majority phase among the ReO_4 salts, so the 2：1 salt is not obtained.)

β -$(BEDT\text{-}TTF)_2PF_6$: 1D along transverse

H. Kobayashi, *Chem. Lett*. **1983**, 581.

Senadeera, *J. Phys. Soc. Jpn*. **67**, 4193 (1998).

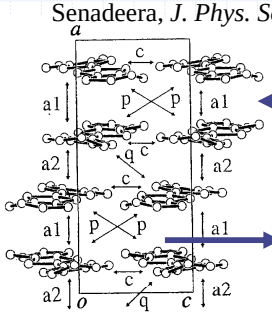

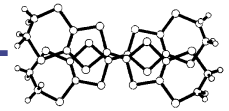

Twisted Dimer構造

Most conducting along this

Open Fermi surface //c

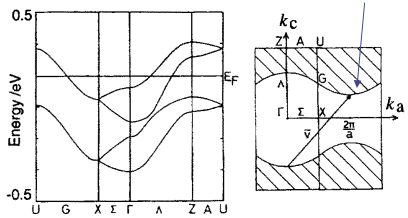

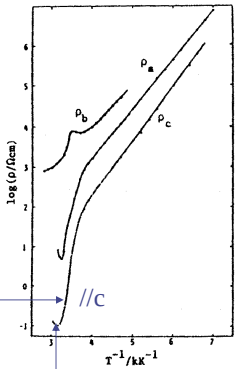

「Peierls」転移@297 K

(2倍周期非磁性絶縁体)

α ‘-$(BEDT\text{-}TTF)_2AuBr_2$:同様

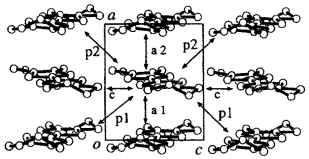

α -$(BEDT\text{-}TTF)_2I_3$

「α 相」起源物質

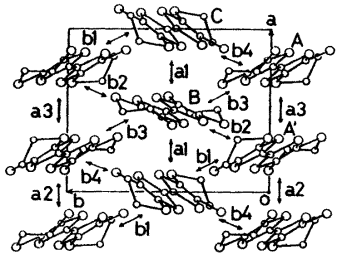

K. Bender, *Mol. Cryst. Liq. Cryst*. **108**, 359 (1984).

T. Mori et al. *Chem. Lett*. **1984**, 957.

Rothaemel, *Phy. Rev*. B **34**, 704 (1986).

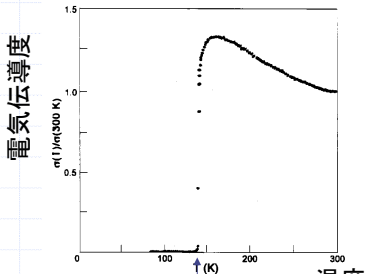

金属-半導体転移@135 K→非磁性絶縁体に。

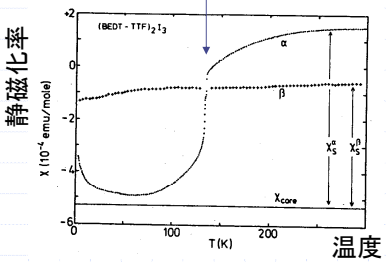

β-$(BEDT\text{-}TTF)_2I_3$

First ambient pressure superconductor based on BEDT-TTF (T_c=1.5 K)。

Yagubskii et al. *JETP Lett.* 39, 12 (1984).

Small pressure increases T_c to 8 K. Murata *JPSJ* **54**, 1236 (1985). Laukhin *JETP Lett*. **41**, 81 (1985).

First 2D close Fermi surface: Mori et al. *Chem. Lett*. **1984**, 957.

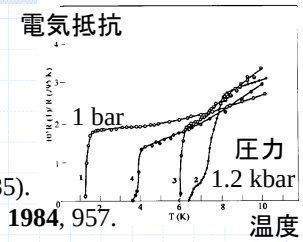

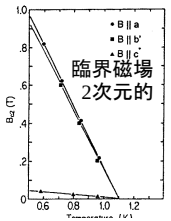

β 構造

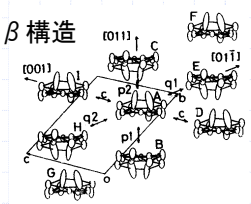

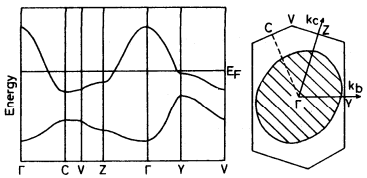

Linear anions AuI_2, IBr_2 other than I_3 make β 型超伝導体 (I_2Br: asymmetry → ×)

$k_BT_c = 1.13\hbar\omega_D \exp(-1/D(E_F)V)$

V: 引力

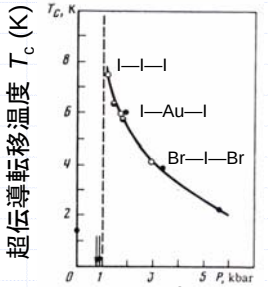

anion 小

単位格子大

状態密度$D(E_F)$大

転移温度T_c大

BEDT-TTF塩:構造分類

Mori, *Bull. Chem. Soc. Jpn*. **71**, 2509 (1998); **72**, 179 (1999); **72**, 2011 (1999).

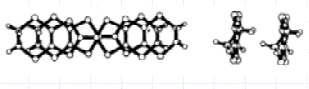

Ring over bond: slip // 長軸方向

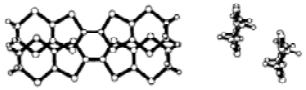

“Ring over atom” slip // 短軸方向

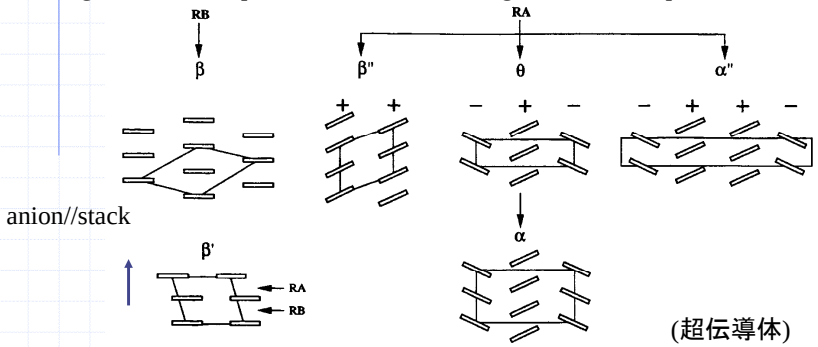

(超伝導体)

Shorter linear anions make β (I_3, AuI_2, I_2Br, IBr_2)→

β ‘($AuCl_2$, ICl_2, IClBr) → β ”($AuBr_2$, ICl_2, AuClBr)

(絶縁体@室温)　　(単純金属@低温, 超伝導×)

電気化学的結晶成長

κ-$(BEDT\text{-}TTF)_2Cu(NCS)_2$

First organic superconductor with exceeding T_c= 10 K (T_c=10.4 K)

Urayama et al. *Chem. Lett*. **1988**, 55; **1988**, 463.

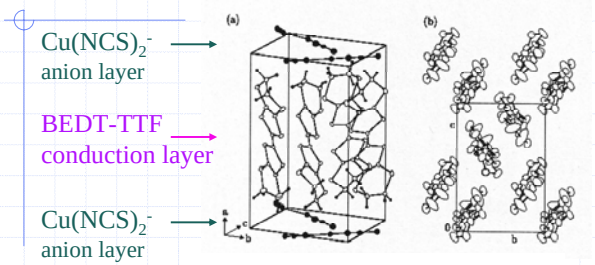

Ideal 2D system

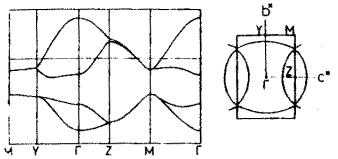

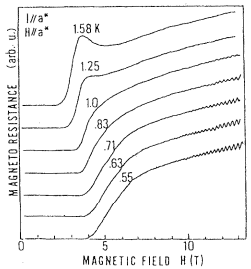

Closed 2D Fermi surface was firstly proved from the observation of Shubnikov de-Haas oscillation.

Oshima et al. *Phy. Rev*. B **38**, 938 (1988).

κ 相統一的相図(鹿野田diagram)

K. Kanoda, *Hyperfine Interact*. **104**, 235 (1997).

κ-$(BEDT\text{-}TTF)_2Cu[N(CN)_2]Br$ T_c=11.6 K

κ-$(BEDT\text{-}TTF)_2Cu[N(CN)_2]Cl$ T_c=12.8 K (0.3 kbar)

J. M. Williams et al. *Inog. Chem*. **29**, 3; **29**, 2555(1990).

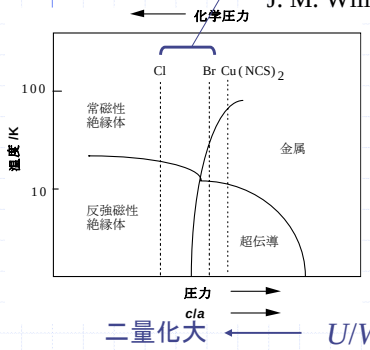

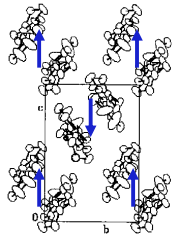

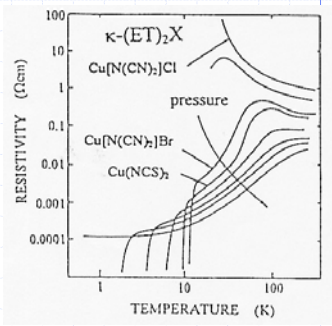

Insulating phase of the κ-phase is a Mott (antiferromagnetic at LT) insulating phase because strong dimerization makes the 1/4-filled band to effectively half filled. Superconductivity appears close to the Mott insulating phase similarly to the copper oxides, suggesting Cooper pair formation related to antiferromagnetic correlation.

α-(BEDT-TTF)$_2$KHg(SCN)$_4$

H. Mori, *Bull. Chem. Soc. Jpn.* **63**, 2183 (1990).
Osada, *Phys. Rev.* B **41**, 5428 (1990).

K→NH$_4$: Superconductor at 0.8 K

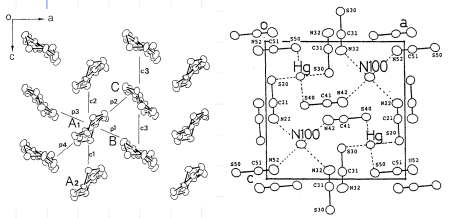

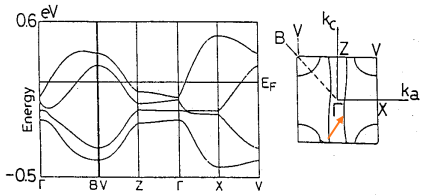

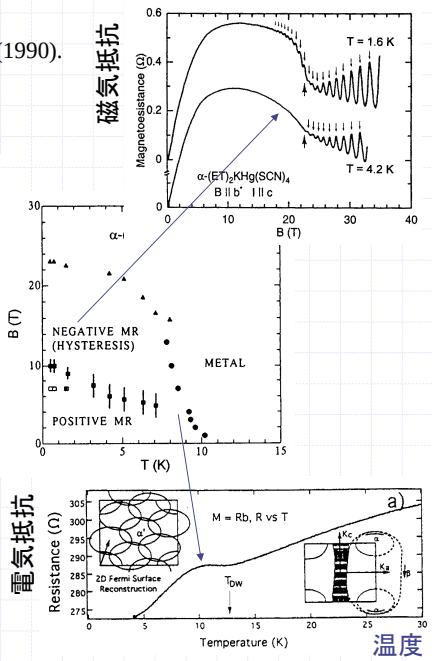

Open Fermi surface makes
CDW or SDW at 8 K

θ 相統一的相図

H. Mori et al. *Phys. Rev.* B **57**, 12023 (1998).

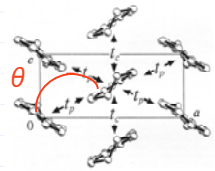

θ-(BEDT-TTF)$_2$MM'(SCN)$_4$

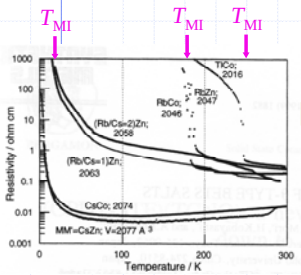

θ-(BEDT-TTF)$_2$MM'(SCN)$_4$

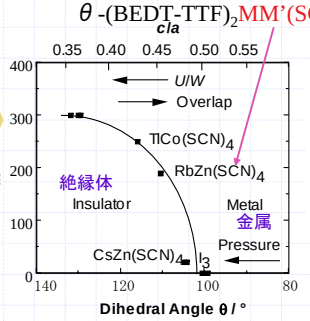

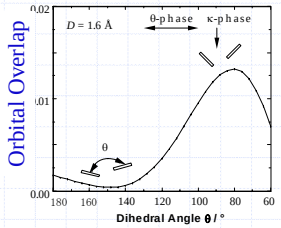

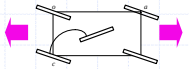

二面角 θ

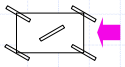

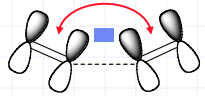

Orbital overlap 大↑

一軸圧縮法→統一的相図検証

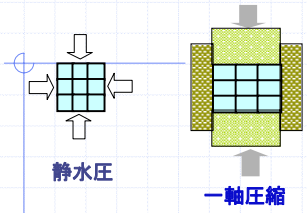

Subtle control different from hydrostatic.
Organics are susceptible to pressure.

Superconducting only under uniaxial strain

- α-(BEDT-TTF)$_2$KHg(SCN)$_4$
- α -(BEDT-TTF)$_2$I$_3$
- θ-(DIETS)$_2$Au(CN)$_4$

θ-(BEDT-TTF)$_2$CsZn(SCN)$_4$

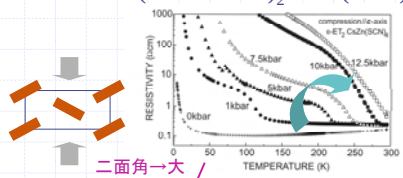

二面角→大

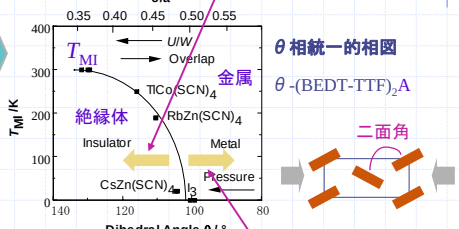

θ 相統一的相図
θ-(BEDT-TTF)$_2$A

二面角

二面角→小

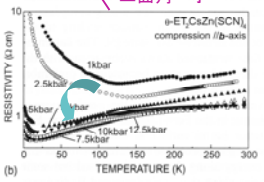

θ 相電荷整列

θ 相：uniform 2次元格子
電荷整列 ← 絶縁化

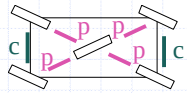

θ-(BEDT-TTF)$_2$RbZn(SCN)$_4$

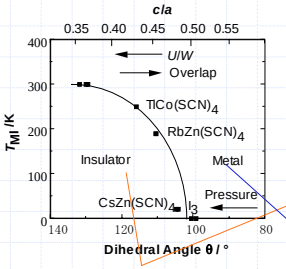

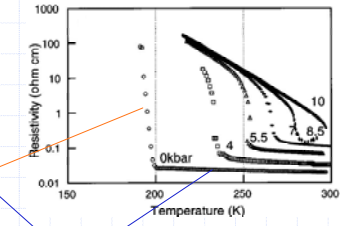

低温絶縁相：電荷整列
Horizontal stripe

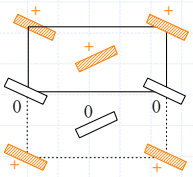

「金属」相：3倍non-stripe
電荷整列 →
平坦電気抵抗
NMR, ラマン, X線
T_{MI}1次転移

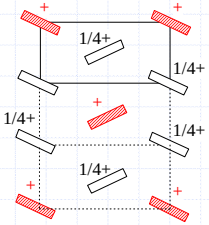

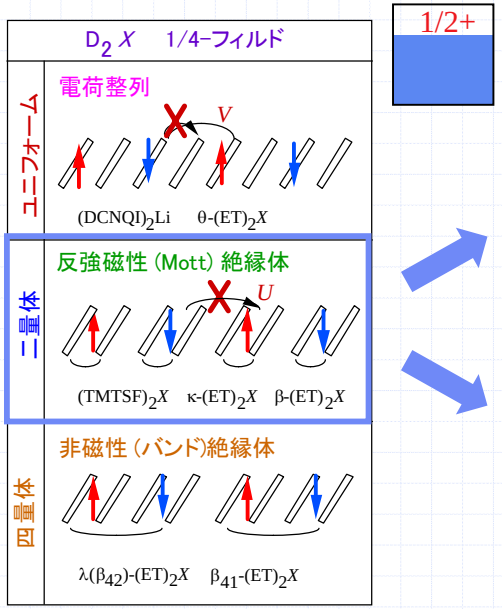

擬一次元系統一的相図

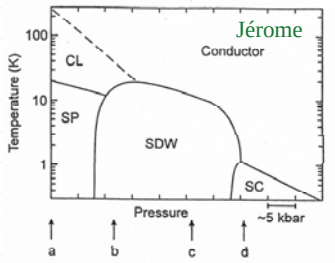

κ 相統一的相図

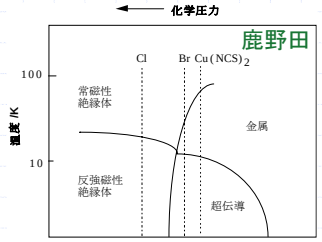

二量化大 U/W

β'- (BEDT-TTF)$_2$ICl$_2$超伝導 T_c=14.2 K (82 kbar) @超高圧下

Taniguchi, et al. *J. Phys. Soc. Jpn*, **72**, 468 (2003).

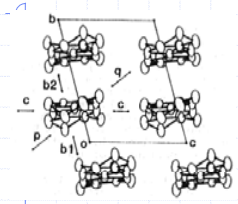

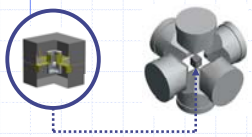

六方anvil

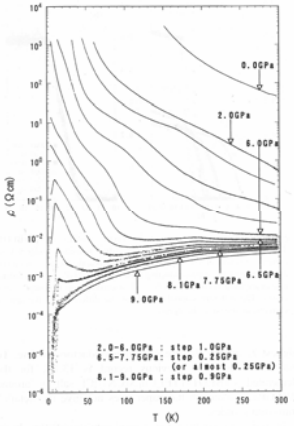

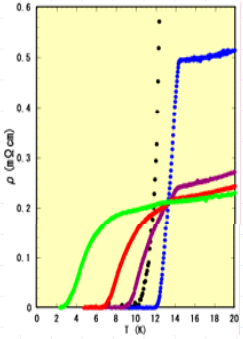

Apply ultra high pressure to a room-temperature Mott insulator to achieve record high T_c.

2:1組成以外有機伝導体

T. Mori, *Chem. Rev*. 104, 4947 (2004).

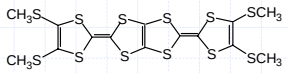

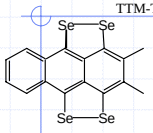

[M(dmit)$_2$]: Only anionic organic superconductor

R. Kato, *Chem. Rev*. **104**, 5319 (2004).

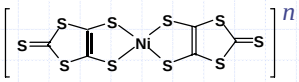

n=0〜2− M=Ni, Pd

(TTF)[Ni(dmit)$_2$]$_2^{1/2-}$
T_c=1.62 K (7 kbar)

((CH$_3$)$_4$N)[Ni(dmit)$_2$]$_2^{1/2-}$
T_c= 5 K (7 kbar)

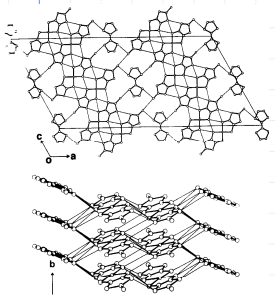

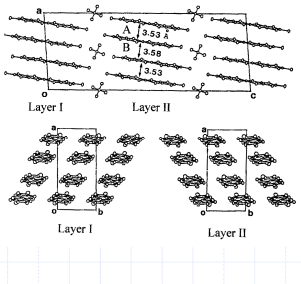

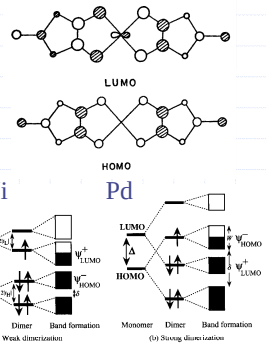

(EDT-TTF)[Ni(dmit)$_2$](1.3 K) is ambient, others are high-pressure superconductors。
1D band. HOMO and LUMO have close energy levels, so that the dimerization (particularly in Pd complexes) leads to crossing HOMO and LUMO bands.

$Cu(DMDCNQI)_2$ Organic conductor coordinated to metals

R. Kato, *Bull. Chem. Soc. Jpn.* **73**, 515 (2000).
S. Hünig, *Chem. Rev.* **104**, 5535 (2004).

1D stack
N of CN coordinate to Cu

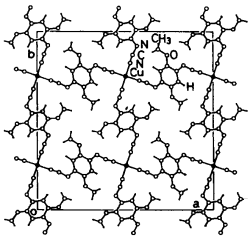

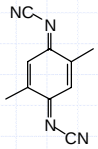

N,N'-dicyano-quinonediimine

DMDCNQI

$Cu^{1.3+}$ mediates interchain interaction to make metallic @LT

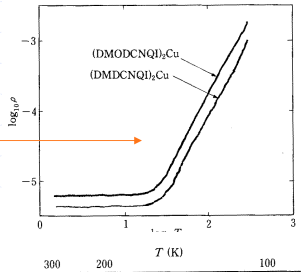

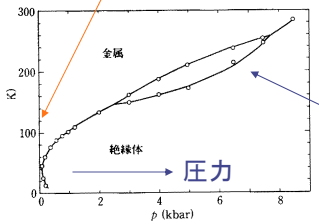

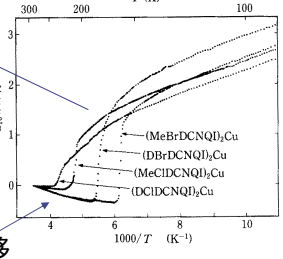

Cu→Li, Na, Ag
→Peierls転移

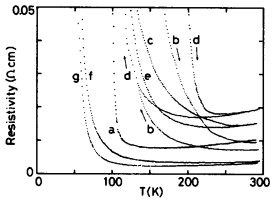

Halogen substituted
DCNQI: 金属-半導体転移

Organic conductors with magnetic anions（π d系）

magnetic anion

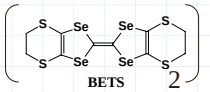

$FeCl_4$

磁場誘起超伝導

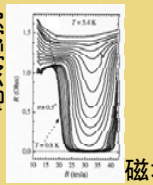

λ-$(BETS)_2FeCl_4$
κ-$(BETS)_2FeBr_4$

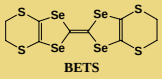

強磁性金属

$(BEDT\text{-}TTF)_3[MnCr(C_2O_4)_3]CH_2Cl_2$

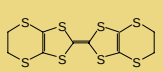

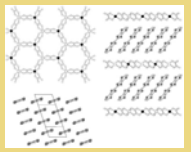

π d系

超伝導と反強磁性の共存

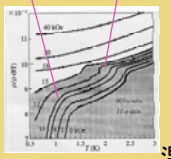

κ-$(BETS)_2FeBr_4$
κ-$(BETS)_2FeCl_4$

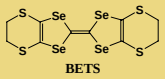

フェリ磁性電荷移動錯体

(Donor) $[Cr(NCS)_4(isoq)_2]$

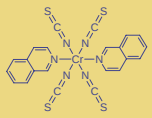

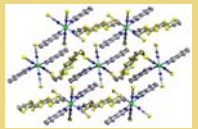

磁場誘起超伝導 λ-$(BETS)_2FeCl_4$

Usually magnetic field destroys superconductivity

In λ-$(BETS)_2FeCl4$, superconductivity appears only at magnetic field.

➡ Comig from the π-d interaction

S. Uji, et al *Nature*, **410**, 908(2001).

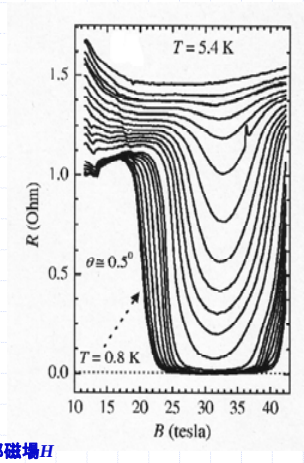

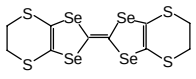

BETS

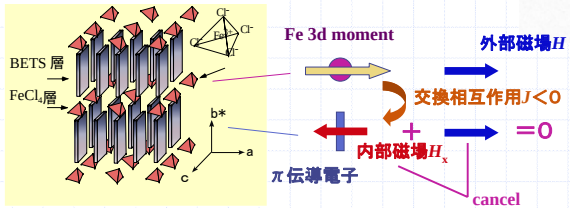

Graphite 層間化合物

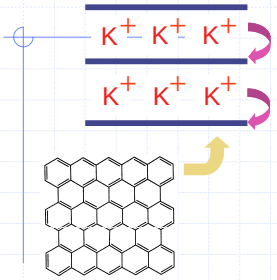

Increase the conductivity

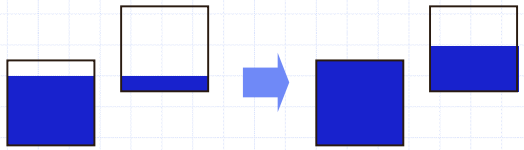

ドープ

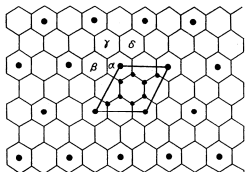

図6 グラファイト・カリウム CaK 中のカリウム原子(●印)の配置

C_8K

Superconducting at very low T
C_8K T_c = 0.39-0.55 K
C_8Rb T_c = 0.03-0.15 K
C_8Cs T_c = 0.02-0.14 K

Energy band of graphite

2次元半金属

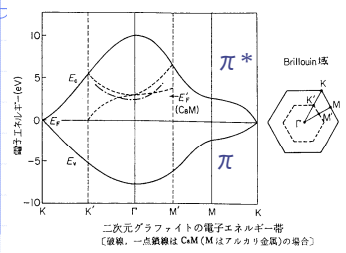

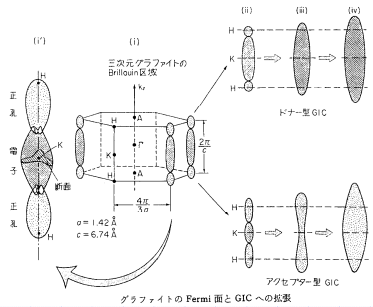

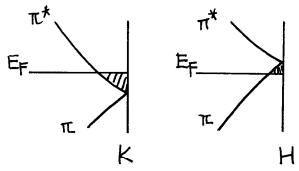

3次元的分子性超伝導体:K_3C_{60}

Fullerene

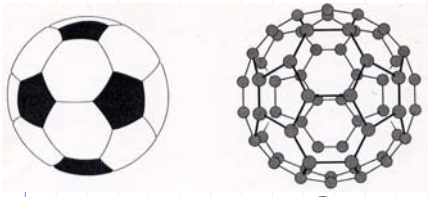

C_{60}

Buckminster Fuller制作Dome

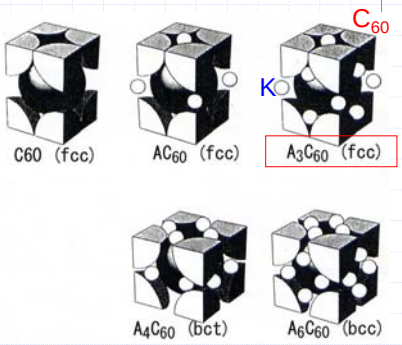

K_3C_{60}分子軌道&超伝導

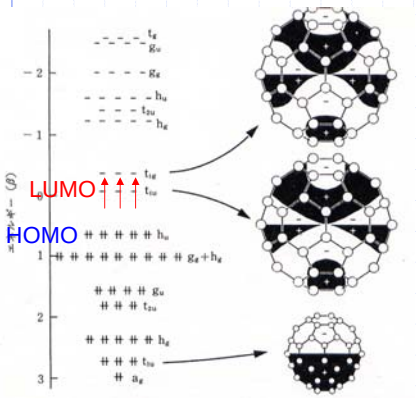

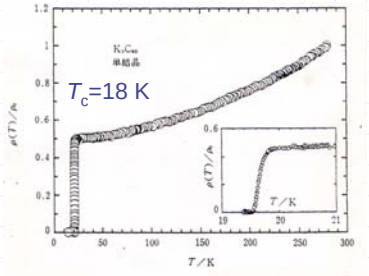

cf. Tc=33K (Cs_2RbC_{60})

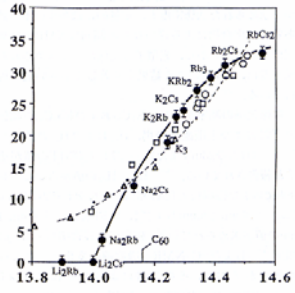

弱結合BCS

$$k_B T_c = 1.13 h\omega_D \exp(-1/D(E_F)V)$$

超伝導物質の転移温度と発見年

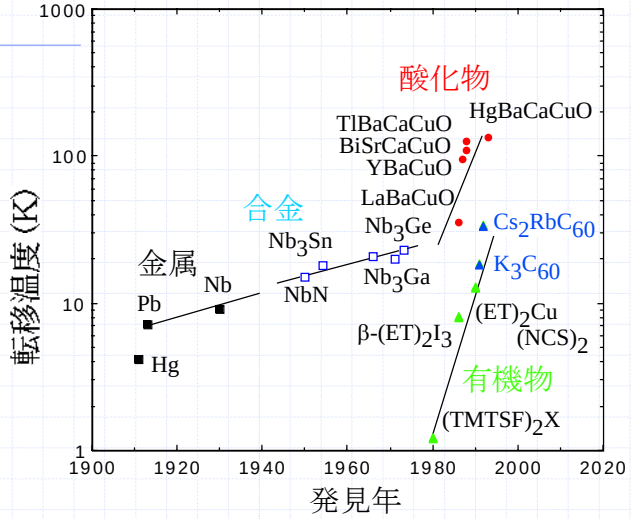

Organic Light Emitting Diode (LED)

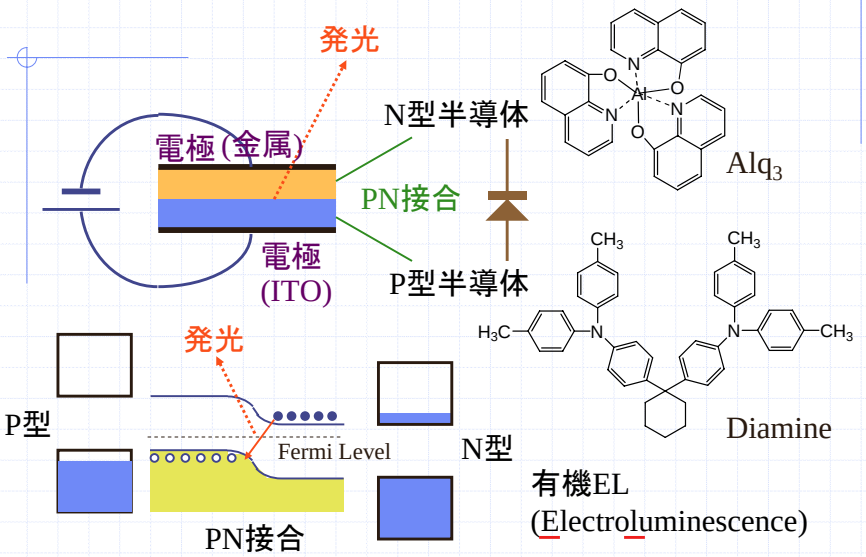

Organic Field-Effect Transistor (FET)

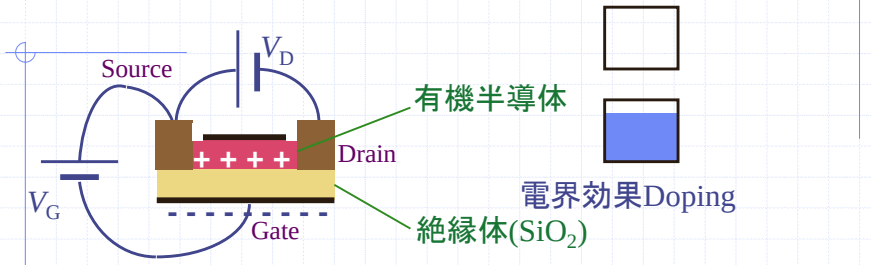

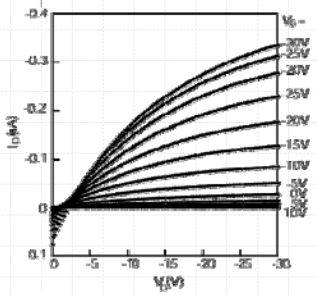

Organic semiconductors for 有機FET

P型

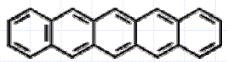

Pentacene

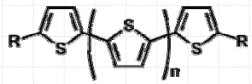

Polythiophene

N型

C_{60}

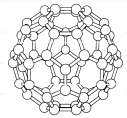

Field-Effect Mobilities

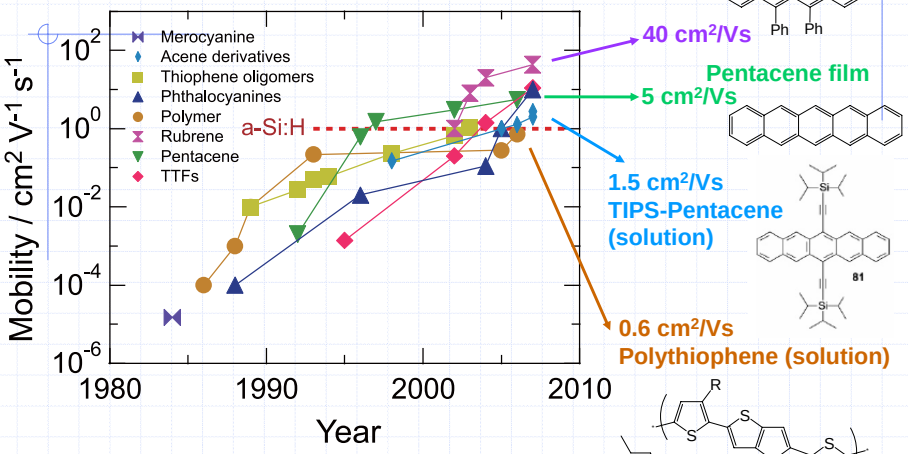

Rubrene crystal

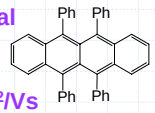

40 cm²/Vs

Pentacene film

5 cm²/Vs

1.5 cm²/Vs
TIPS-Pentacene
(solution)

0.6 cm²/Vs
Polythiophene (solution)

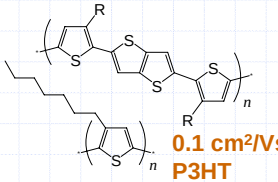

0.1 cm²/Vs
P3HT

T. Mori, *J. Phys. Cond. Matter*. **20**, 184010 (2008).

A. R. Murphy and J. M. J. Frechet, *Chem. Rev*. **107**, 1066 (2007).

Structures of Organic Semiconductors *Acta Crystallogr*. B **45**, 473 (1989).

Herringbone (θ-type): large side

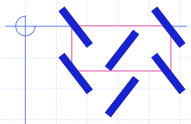

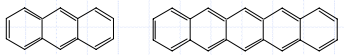

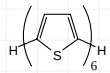

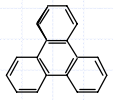

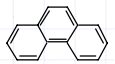

phenanthrene

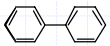

biphenyl

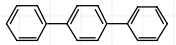

terphenyl

Dimer (κ-type): intermediate

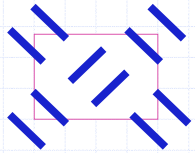

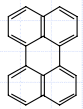

perylene

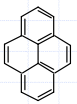

pyrene

γ-構造(θ-type): large plane

Stack (β-type): large plane

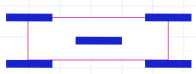

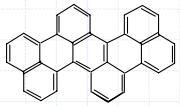

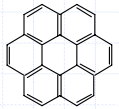

coronene

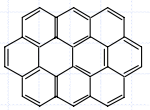

ovalene

Large plane reduce the tilting angle.